AD-A090 429 ARMY MATERIALS AND MECHANICS RESEARCH CENTER WATERTOWN MA F/G 11/4
LASER INTERACTION WITH TBR MATERIALS,(U)
JUN 80 J S PERKINS

UNCLASSIFIED NL

END
DATE FILMED
11 80
DTIC

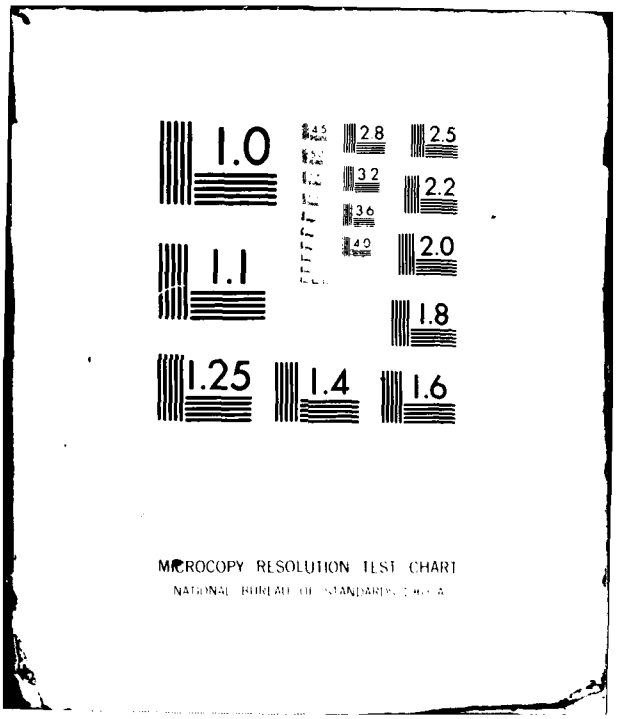
1.0
1.1
1.25
1.4
1.6
1.8
2.0
2.2
2.5
2.8
3.2
3.6
4.0
MICROCOPY RESOLUTION TEST CHART
NATIONAL BUREAU OF STANDARDS

LASER INTERACTION WITH TBR MATERIALS

JANET S. PERKINS, Ph.D.
ARMY MATERIALS AND MECHANICS RESEARCH CENTER
WATERTOWN, MASSACHUSETTS 02172

In a number of areas the Army has need for high-temperature, heat-shielding materials that retain shape and structural integrity in severe thermal environments. Some applications are the throat of a jet engine or the interior of a rocket combustion chamber.

We have been examining the response of a number of composite materials to a high-energy-flux environment using a welding laser instead of the arc furnaces of earlier studies. A laser is a clean, well-defined energy source. If used with an air stream or an exhaust system to remove pyrolytic products and debris, we can isolate the action of energy flux from secondary effects and reduce scatter in data.

Typical of the structural forms we have tested are foams, fabric-reinforced composites and bulk graphite. Silica or carbon microballoons or fabric reinforce the newer high-temperature resins in samples we have compared with ATJ and pyrolytic graphites.

A sampling of ablation results are shown in Table I. Among these materials, two are outstanding, both as thermal barriers and in retention of structural integrity. These are pyrolytic graphite and TBR. The former is a form of bulk graphite deposited at high-temperature on a substrate from a carbonaceous gas, e.g., methane. The latter is a relatively new material fabricated from carbon cloth and a Hitco proprietary resin. Both have a laminar structure.

FABRICATION OF TBR

The class of materials known as TBR, an acronym for tungsten-bearing resins, is made by impregnating layers of carbon cloth with a resin containing tungsten atoms chemically bound within the polymer backbone. The laminate is then cured, carbonized, and fired to a graphitizing temperature producing a carbon in tungsten carbide composite. At this temperature, the tungsten carbides sinter and bond the layers of carbon fabric together.

The outstanding behavior of TBR composites has raised questions as to how and why it outperforms other composites as well

as bulk graphites. Our research has focused on finding answers to allow tailoring of new composites for special applications.

After analyzing the system in depth both during and after irradiation, we conclude that the excellent performance can be attributed to the following sequence of events:

(1) The 10.6-μm beam produced by the CO_2-laser caused the carbon to become incandescent, reradiate a substantial fraction of its energy, and become very hot (3300°C).

(2) The heat causes the sintered tungsten carbides to melt and coat the carbon fibers with (a) a protective layer against air erosion, (b) a reflecting and heat-conducting surface layer, and (c) a reactive layer for transport and escape of atomic carbon from the underlying carbon fabric.

This paper presents evidence for these conclusions and shows why this system is inherently able to interact with very high intensity radiation with minimal structural damage.

TABLE I. ABLATION VALUES OF COMPOSITE MATERIALS [a]

Material	Reinforcement/Matrix	Density(ρ) g/cc	Exposure(t) sec	Depth of Burn(d) cm	Q^* kJ/g
Syntactic Foams	SiO_2-MB/ polyimide	0.38	2.5	3.8	18
	C-MB/ polyimide	0.30	2.5	3.8	23
	C-MB/ H-resin	0.78	1.9	0.5	51
Woven Fabric Laminate	SiO_2/ phenolic	1.77	3.6	1.3	17
	Nylon/ phenolic	1.02	5.5	2.6	22
	C/TBR	2.18	5.5	<0.10	>200
Bulk Carbon	Pyrolytic graphite	2.20	5.5	0.14	200

[a] Exposed to CW CO_2-laser ($I=10.5$ kW/cm^2) which was essentially monochromatic (10.6μm).

[b] Ablation values based on surface recession calculated by: $Q^* = \frac{It}{d\rho}$. With the exception of TBR and pyrolytic graphite, the exposure times are burn-through times.

(114)

PERKINS

CHARACTERIZATION OF TBR

The 1/8-inch thick material used in these experiments contained 19 layers of a satin-weave carbon cloth. It was bonded with Hitco proprietary resin, TBR-1, and fired to 2800°C.

X-ray diffraction analysis of the final product shows the broad carbon bands typical of carbon cloth (Figure 1a) underlying spectra of the three quenched high-temperature forms of tungsten carbide, W_2C, β-WC_{1-x}, and WC, (Figure 1c) as well as several of the more prominent bands of graphite. The resin alone, heated to 2800°C, gives a spectrum notable for its lack of β-WC_{1-x} and the predominance of W_2C (Figure 1b).

Examination of the phase diagram (1) for the tungsten-carbon system gives insight into the X-ray diffraction pattern of the fired resin (Figure 2). Analysis of this resin shows a large molar excess of carbon over tungsten which presumably would favor the formation of WC rather than the predominance of W_2C found. However, at 2780°C, WC melts peritectically to give solid carbon and a liquid phase rich in W from which W_2C precipitates on cooling. Absence of any of the bands of β-WC_{1-x} found in the laminate is not surprising since this is stable only above 2530°C.

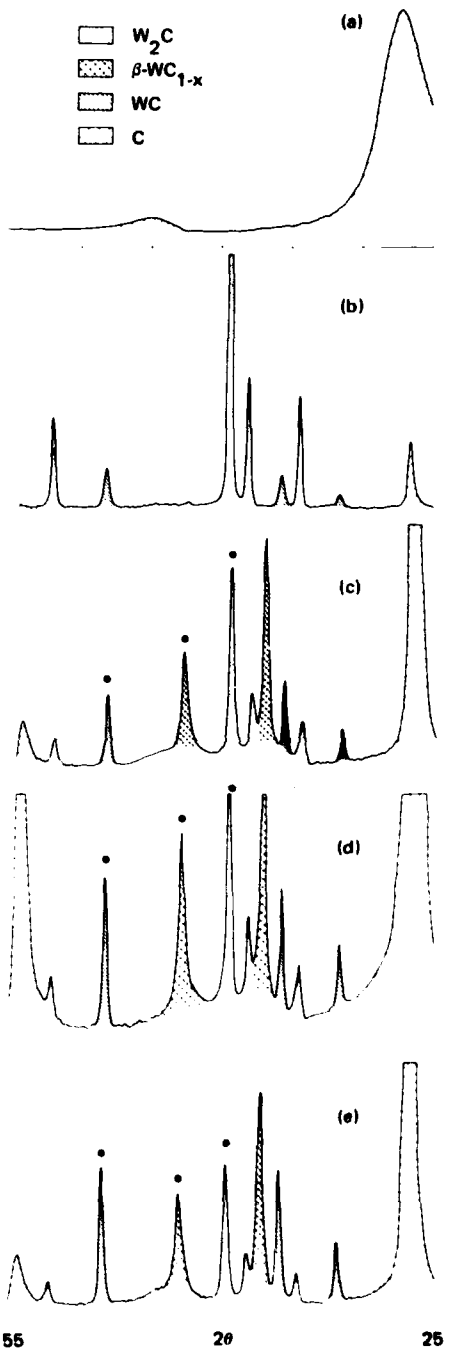

Figure 1. X-ray diffraction scans of TBR constituents and of TBR before and after CO_2-laser irradiation: (a) carbon cloth, (b) fired TBR-1 resin (2800°C), (c) TBR, as-received, (d) after 10 kW/cm^2 irradiation, (e) after 30 kW/cm^2 irradiation.

(115)

When the fired resin remains in intimate contact with the carbon-cloth substrate at the high firing temperature for an extended period, the three high-temperature carbides will accumulate in the steady state and persist in the quenched product. These result from the high-temperature reversible redox reactions:

$$W_2C + C \rightleftharpoons 2\beta\text{-}WC_{1-x} + xC \rightleftharpoons 2WC \qquad (1)$$

This is the evidence on which we base our description of the starting material as carbon cloth layers held together by sintered tungsten carbides and carbon from pyrolysis of the original tungsten-containing polymeric system.

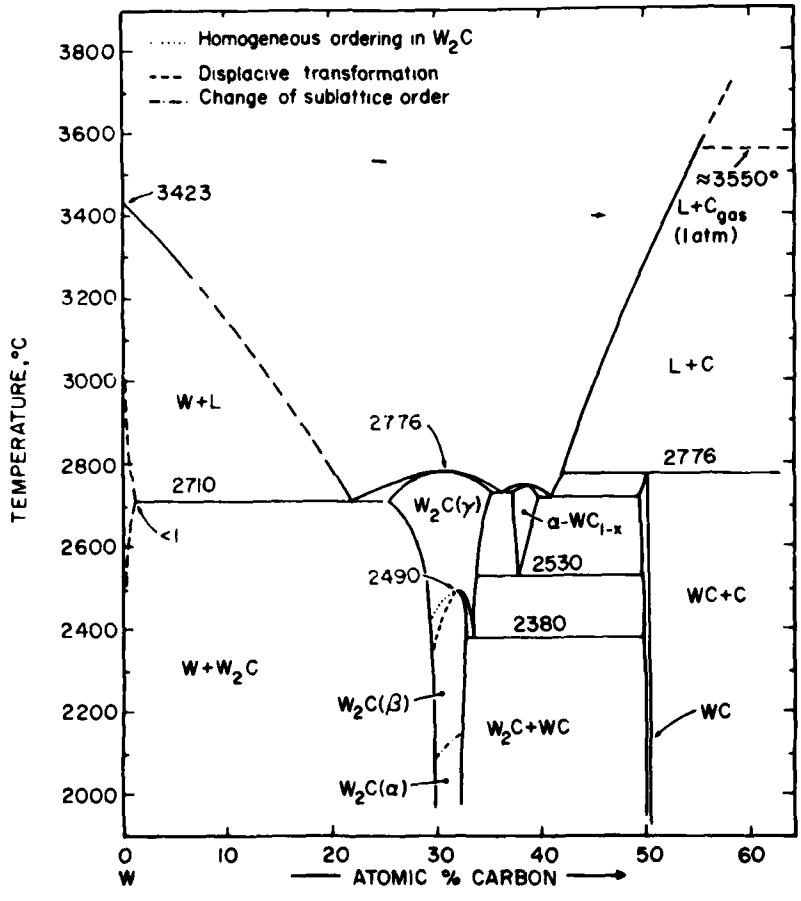

Figure 2. **Binary phase diagram of the tungsten-carbon system.**

EVIDENCE FOR CHEMICAL CHANGES DURING IRRADIATION

X-Ray Diffraction

The surface composition of the material irradiated by lasers (10 and 30 kW/cm^2) shows shifts in the ratios of W_2C and WC relative to β-WC_{1-x} (Table II). There has been a shift to the right in reaction (1).

TABLE II(U). RELATIVE CHANGE IN AMOUNTS[a] OF QUENCHED TUNGSTEN CARBIDES WITH LASER INTENSITY

	Original	10 kW/cm^2	30 kW/cm^2
W_2C	1.88	1.31	0.87
WC	0.73	0.86	1.17

[a]Ratios of W_2C and WC to β-WC_{1-x} based on peaks (•) in Figure 1c-e.

The shift to larger concentrations of WC, the higher the laser intensity, is a reasonable effect. The increased energy flux speeds up both the escape of carbon vapor from the thin tungsten carbide surface layer as well as reaction of this hotter layer with the carbon substrate to give a net equilibrium shift toward WC.

Microscopy

At this stage in the argument, it is worthwhile to examine photomicrographs of both samples (Figure 3). The high-intensity beam

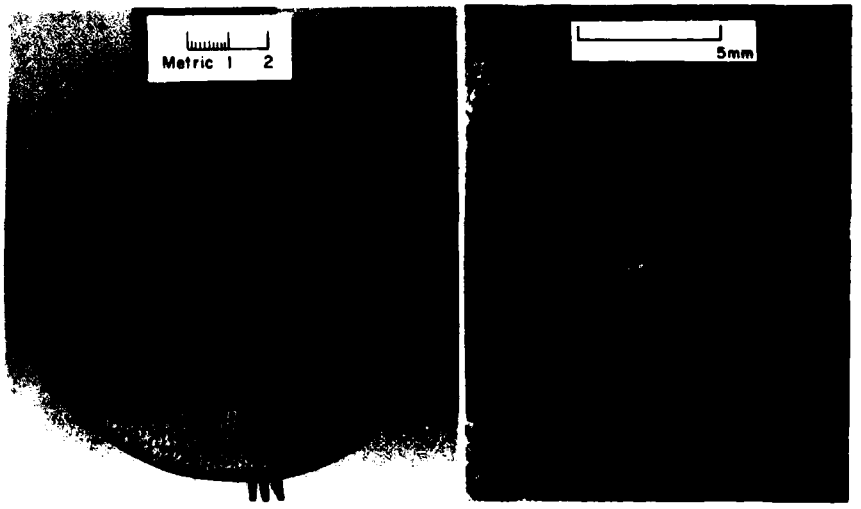

(a) (b)

Figure 3. (a) 10 kW/cm^2 burn on 1/8-inch disk of TBR (5.5 sec.); (b) cavity in second disk after burn-through of top 1/8-inch disk by 30 kW/cm^2 CO_2-laser (5 sec.).

(117)

cut through the upper of two stacked disks and penetrated the lower; the low intensity beam barely penetrated the top layer of the first disk. In the scanning electron photomicrographs, (SEM) of the low intensity burn shown at three magnifications (Figure 4), a semiliquid phase is just beginning to coalesce. (The tiny dot in a is enlarged in b). The related EDAX micrograph c of the semifluid edge, enlarged in d, shows the distribution of tungsten as white dots, indicating great enrichment of tungsten in the semiplastic matrix though carbon features still persist. Note the carbon fiber stubs marked by arrows in c and d.

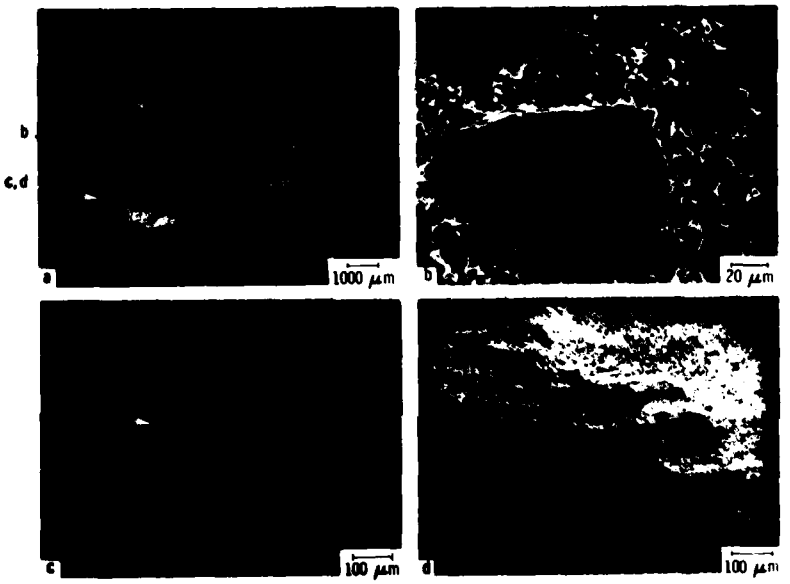

Figure 4. Scanning electron micrographs (SEM) and energy dispersive analysis by X-rays (EDAX) of TBR irradiated by 10 kW/cm^2 CO_2-laser (a) SEM of burn area, (b) enlargement of microdroplet, (c) EDAX of burn edge, (d) SEM of same area.

The high-intensity laser cut deeply and slowly into TBR and vaporized the carbon fabric, leaving shiny drops of molten, metallic tungsten carbides on the walls and at the forefront of the cavity (Figure 5). Near the mouth of the cavity, two or more phases are clearly evident on the surface of these drops (Figure 5a and d) and the EDAX photomicrograph showing the distribution of tungsten (Figure 5b) verifies the enrichment of W_2C in the surface coat of WC as C escapes.

(118)

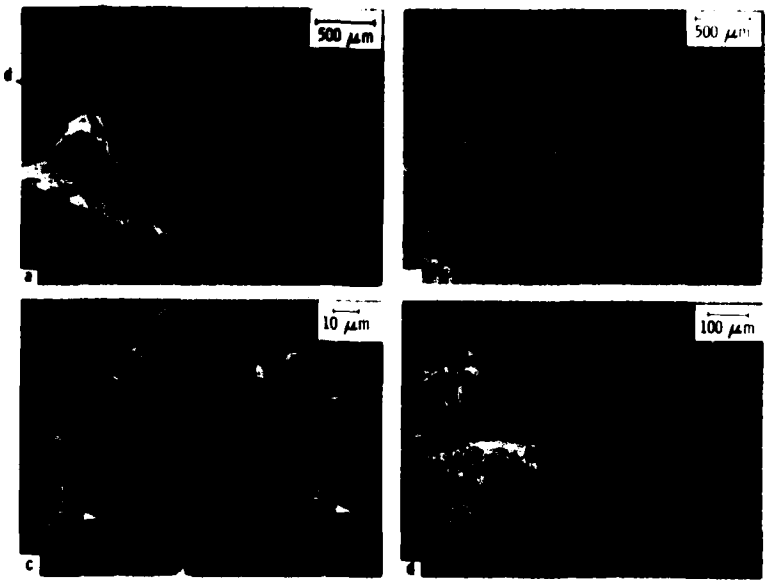

Figure 5. Scanning electron and energy dispersive photomicrographs of TBR irradiated by 30 kW/cm^2 CO_2-laser: (a) SEM of mouth of burn cavity, (b) EDAX of same area, (c) fibers from midpoint of burn showing (1) redeposition of carbon, and (2) residual coating, (d) enlargement of tungsten carbide drop showing carbon deficient upper layer.

The SEM of a group of fibers from the wall area halfway down the burn (Figure 5c) has two features of interest: the bulbous growth of carbon at 1, and the residual tungsten-rich sheath at 2 which previously surrounded a fiber now eaten away. Both are evidence of the occurrence of the peritectic reaction

$$2WC \longrightarrow W_2C + C \qquad (2)$$

producing the disappearance of fiber with redeposit of some vapor in a cooler portion of the sharp thermal gradient.

LASER ENERGY ABSORPTION THROUGH CHEMICAL REACTION

The significance of these observations becomes apparent when we consider the related thermodynamic data as well as the mechanisms by which the relatively low-energy photons in a CO_2-laser can interact with a carbon-fiber reinforced tungsten-carbide matrix.

Thermodynamics

Let us first examine the thermodynamics of the proposed system. The only high-temperature data we have found gives formation enthalpies at 2800°C for W_2C and WC (2). Gupta and Seigle (3) determined the heat of formation and free energy of W_2C at 1300°C below which it is unstable. WC is the only thermodynamically stable form of tungsten carbide at room temperature.

For equilibrium or steady state conditions at 2800°C, calculated heats of reaction for solution and vaporization of carbon give a net absorption of 170 kcal/mole of C:

	ΔH, kcal/mole
$C(s) + W_2C \longrightarrow 2WC$	-5
$2WC \longrightarrow W_2C + C(g)$	175
$C(s) \longrightarrow C(g)$	170

(3)

which translates to 60 kJ/g of carbon volatilized and indicates a highly endothermic system. The actual energy absorption must be greater under laser irradiation by reason of the following:

No account is taken in our energy calculations of the heat of melting the W_2C and WC (no data available).

A nonequilibrium system during irradiation corresponds to a higher energy input and a higher temperature for reaction than that measured on a system infinitesimally removed from equilibrium, i.e., conditions under which thermodynamic data are measured.

The emissivity of the tungsten carbide system is not known at the face temperature recorded (3230°C) for which the emissivity was assumed to be 0.999. The true temperature must be several hundred degrees higher, judging from emissivity measurements made in our laboratory from 700-1700°C on TBR material;* the normal spectral emissivity diminishes from 0.85 to 0.72 in this interval. The normal spectral emissivities of W_2C, WC, and pyrolytic graphite at 0.9μm, (the wavelength observed by the optical pyrometer during our experiments) are listed by Touloukian as 0.48 (2130°C), 0.59 (1530°C), and 0.79 (1780°C) (4).

*Private communication from K. J. Tauer.

(120)

PERKINS

Crystallography

We have assumed that monoatomic carbon is the principal volatile species from WC whereas the volatile species from graphite contain a number of polyatomic species -- C_2, C_3,...C_6, ...(5). Per gram atom, the formation of C absorbs the largest amount of energy; all bonds to neighboring atoms are broken.

With carbon release from WC, there is good reason to believe that the initial species evolved is the more highly energetic C_1 as suggested by earlier workers (6). Some aspects of carbon removal from the tungsten carbide lattice, whether solid or molten, can be deduced by examining the crystal structure of WC (Figure 6). In general, the X-ray diffraction patterns of liquids near the melting points show the same short distance order as the parent crystals (7). From two neighboring WC cells, carbon atoms are released at distances greater than the C-C bond distance in graphite (1.67Å vs 1.42Å). Unless a carbon atom (or ion) rolls across the electron surface cloud to bond with another emerging C_1, C_2 should not be observed in the vapor. If present, it must be a secondary product.

Further support for this view of single carbon atom egress from the WC lattice at 2800°C or above is found in the elegant study by French of carbon atom diffusion into the tungsten body-centered cubic lattice at 1000°C (8). He photographed, by field ion microscopy, the atomic positions of W atoms in the successive layers of the tip of a carburized tungsten wire as these layers were removed one by one. This remarkable series of photomicrographs passes from the WC surface to the underlying W crystalline state. By observing the shift in the positions of the tungsten atoms, made visible by

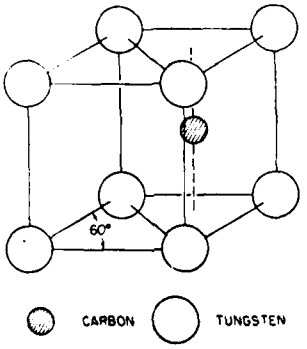

Figure 6. Hexagonal unit cell of WC.

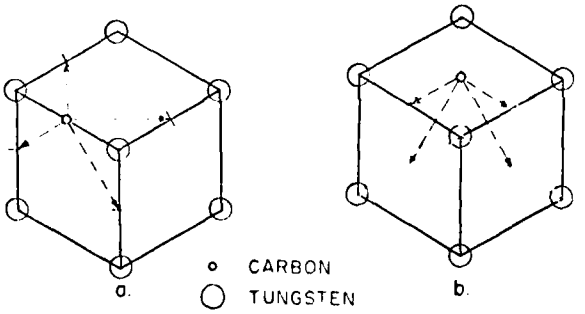

Figure 7. Transport of carbon atoms through tungsten body-centered cubic lattice [after French (8)].

(121)

this technique, he concluded that the diffusion of carbon into and through the tungsten lattice proceeded by single atoms entering either the edge or the face of the unit cells on the surface, followed by passage within the cells from edge to inner edge or from face to inner face (Figure 7).

The phenomenon that we have trapped in the thin skin of tungsten carbides overlaying the carbon fibers corresponds to the reversal of carbon diffusion -- from carbon fiber, in this case, through the thin tungsten-carbide skin to the surface.

Let us consider the fate of the released single carbon atoms. Those emerging with sufficient energy to escape from the surface can be oxidized or can redeposit downstream either to build pyrolytic graphite or amorphous soot. Those with lesser energy can travel across the surface to a cooler area where a well-crystallized graphite ring is forming. We have evidence for both. In either case, the net energy required to produce these single carbon atoms from the underlying graphite fibers must be greater than the thermodynamic value to atomize graphite given in Equation 3.

As is clearly visible in Figure 8, the high-energy laser burn is surrounded by a border of pyrolytic carbon in well-formed graphite layers. Low-intensity laser burns also are surrounded by pyrolytic carbon. The movies of samples during irradiation show

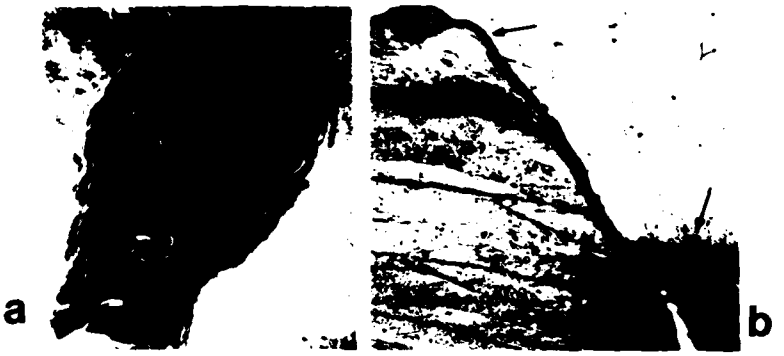

Figure 8. (a) SEM of portion of carbon ridge around 30 kW/cm^2 burn and (b) polished metallographic mount of burn cavity cross section showing solid- and open-layered structure of ridge, and large drop of tungsten carbides at lower right.

(122)

intense incandescence of these rings as the atomic building blocks release their energy. By contrast, the centers of these burns appear relatively cool.

When a block of pyrolytic carbon is irradiated, the entire burn area and the overlaying plume become incandescent due to polyatomic species. These seem to be absent when TBR is irradiated.

From these observations and arguments, it may be concluded that the energy required to release carbon must exceed that required to separate the original carbon lattice into atoms.

UNIQUE FEATURES OF TBR

Stability of Carbide Matrix: 3000° Liquid Phase

Physical Constants

At this point in the argument, some observations on stability are in order. Among all elements, carbon has the highest melting point (3652 or 3870°C) and a very high boiling point (4200°C) (9). These signify the strongest interatomic bonds between atoms of any element as well as strong lattice bonding. Tungsten, with the next highest melting point (3400°C) and somewhat weaker lattice bonding, has a higher boiling point (5530 or 5900°C) (9) and shows very strong interatomic bonding.

Most significant, however, are the melting and boiling points of the binary tungsten carbides. The three high-temperature crystallographic phases all melt within 30±12 degrees and the three associated eutectic compositions within the 40-degree interval below this. This means that the tungsten carbides melt sharply at about 2750±30°C, nearly 1000 degrees below the melting point of carbon and 600°C below that of tungsten (Figure 2). The boiling point of the tungsten-carbon "alloy" is listed as greater than 6000°C, higher than that of any other compound. What is particularly significant about this 3000°C liquid range is the relative permanence of the liquid state as the solid substrate vaporizes through it. Also indicated is the stabilizing effect of carbon atoms intermingled with tungsten in the liquid phase; the liquid phase remains well above the boiling points of either constituent.

Wetting of Fibers

A second significant property of the tungsten-carbon "alloy" that we have observed, is that once molten, it wets the carbon fibers of the cloth very well. Silvery bundles of fibers were separated from the sawdust of the sample irradiated with the higher intensity laser, which was sawed in half before mounting. These came from the

(123)

cylindrical area near to and surrounding the burn-hole to which the molten, reactive matrix had been driven. The molten coating (a) improved the contact of the C-W_2C reactants, (b) protected the hot carbon fabric from reactive gases such as CO, CO_2, or O_2, and (c) on solidifying, "mechanically hardened" the structure. The mechanical hardness of tungsten carbides is well known.

What we observe, then, in the interaction of the high-intensity 10.6μm laser and TBR is a highly endothermic "redox" reaction of liquid tungsten carbides with solid carbon, initially supplied by the pyrolyzed resin, then by the reinforcing fabric itself. There is also a fluid flow inward of the reacting matrix to give a permanent hard bond on cooling. Additionally, some of the released carbon redeposits as pyrolytic carbon around the periphery of the burn; this also increases the mechanical strength of the damaged piece.

Laminar Structure

Radial Energy Dissipation

There are further aspects of the burn residues shown in the polished metallographic section in Figure 8 that elaborate this mechanism. The only two to which reference will be made are the following:

> Because of the very low volatility of tungsten carbide even as carbon is diffusing through it, the atoms of tungsten remains in or near the burn area. The laser energy is chiefly dissipated by vaporizing monatomic carbon.
>
> Because of the laminar structure of the TBR material tested (as is also true of the pyrolytic graphite similarly irradiated in our tests), penetration of energy normal to the surface is minimal; energy not absorbed by the reaction or by reradiation is dissipated laterally by conduction within the upper layers only.

Skin Effect

Another unusual aspect of TBR may be called a "skin effect." This was observed in monitoring both TBR and pyrolytic graphite samples during irradiation. We believe this effect accounts for the peculiar patterns of soot deposited on these surfaces and certain anomalies in the surface-temperature records made during laser irradiation. It appears to contribute significantly to the barrier action of TBR.

(124)

(a) (b)

Figure 9. Five-second 10 kW/cm^2 burns on (a) TBR and (b) pyrolytic graphite (0.1 Mach wind tunnel).

Figure 9 shows burns of both TBR and pyrolytic graphite which were mounted in a 0.1-Mach wind tunnel and irradiated with a 10 kW/cm^2 laser beam. The similarity in soot patterns is striking. Both patterns appear to originate at or near the edge of the molten or plastic face of the burn area. These figures verify that the soot source is at the edge of what high-speed movies indicate is a lifting of a cohesive but plastic surface due to carbon vapor build-up below as well as above the upper-most laminae. Trapped below this blister, the carbon vapor has a chance to coalesce into soot mixed with other condensed carbon fragments until the vapor pressure becomes great enough to slit the blister or tear the edge in the weakest area and release the trapped mixture.

With pyrolytic graphite in two successive runs, the breaking of the plastic "skin" was quite visible on the video scan monitor as well as in the movies. A white incandescent bulge appeared, tore at the right edge, lifted up and burned back from the reactive broken edge exposing a much cooler, black underlayer which, in turn, became incandescent, lifted, and similarly disappeared. In one run, this occurred twice; in the other, three times. The rise and fall of the recorded front surface temperatures, twice and three times, verifies the observations. The front face temperature recorded with TBR was considerably lower and has a shallow wave form consistent with the more fluid or plastic top laminate during irradiation.

Multiphoton Absorption: Initially by Carbon

This discussion would be incomplete without some remarks about the initial stages of irradiation. Each mole of photons in the 10.6μm laser beam carries only 2.7 kcal (0.9 kJ) of equally distributed energy. This energy is only sufficient to initiate restricted, rotational motion of one C-C bond per photon absorbed. Each bond must absorb many quanta of this energy to approach the energies for bond vibrations, for electronic transitions resulting in light emission, and ultimately for bond breaking or the initiation and support of an energy-absorbing chemical reaction.

(125)

One observation from the high-speed movie record of a sample of TBR is that the first frame showing a visible change occurred 1.41 seconds after the start of laser action and showed the cross-hatch appearance of the incandescent carbon fabric just as the matrix melted. In the next frame, this was obliterated in the overall incandescence of the fabric and matrix. This supports the belief that carbon, rather than the tungsten carbides, is capable of absorbing significant amounts of radiation at 10.6μm. This is a requirement for interaction of photons with matter.

From these data and observations, we conclude that the sequence of reactions is the following:

- Multiphoton absorption of 10.6μm radiation by carbon to raise it to incandescence and a sufficiently high temperature to soften the tungsten-carbide/carbon matrix.
- Initiation of rapid carbon migration from solid carbon through the tungsten carbide matrix to the liquid-vapor phase boundary in a highly endothermic process.
- Escape of hot atomic (or ionic) carbon either from this surface as vapor or across this surface to produce an incandescent pyrolytic graphite ring.
- As a concomitant reaction, lifting of the top layer of the laminate intermittently to release clouds of soot and vapor which have cushioned lower layers from direct conductive heat transfer.

SUMMARY

To recapitulate and add some corollaries, the damage-limiting mechanisms provided by TBR under CO_2-laser irradiation include:

- reradiation of higher energy photons by multiphoton-activated carbon;
- reflection of substantial fractions of laser energy as the tungsten carbide both on and under the surface laminate becomes molten;
- protection of carbon fabric from air erosion by the molten matrix;
- lateral energy transfer through molten carbide-coated carbon fabric layers;
- limitation of energy transfer from layer to layer by protective blister formation;

(126)

- intermittent detachment of radiating reacting layers from the substructure;
- the highly endothermic, renewable reaction system of tungsten carbides and carbon which facilitates a smooth, relatively slow burn;
- mechanical strengthening of the burn area in this laminar material by transport and resolidification of the molten matrix and deposit of pyrolytic graphite in the vicinity of the laser burn.

We submit that this analysis defines the major sequence of events that occur when TBR is irradiated by a CO_2-laser and that it provides a reasonable model to explain the outstanding thermal response of this material.

REFERENCES

1. E. Rudy, "Ternary Phase Equilibria in Transition Metal-Boron-Carbon-Silicon Systems," Part V, AFML-TR-65-2, Air Force Materials Laboratory, June 1969, p. 192.
2. H. L. Schick, "Thermodynamics of Certain Refractory Compounds," Vol 2, Academic Press, New York, 1966, pp. 83, 85.
3. D. A. Gupta and L. L. Seigle, Metall. Trans., 6A, 1939 (1975).
4. Y. S. Touloukian and D. P. DeWitt, "Thermophysical Properties of Matter," Vol 8, IFI/Plenum, New York, 1970, p. 830.
5. H. B. Palmer and M. Shelef, "Vaporization of Carbon," Chemistry and Physics of Carbon, Vol 4, Marcel Dekker, Inc., New York, 1968, p. 129.
6. E. K. Storms, "The Refractory Carbides," Academic Press, New York, 1961, p. 154.
7. M. A. Omar, "Elementary Solid State Physics," Addison-Wesley Publishing Co., Reading, MA, 1978, pp. 21-23.
8. R. D. French, PhD Thesis, Brown University, Providence, RI, 1967.
9. G. V. Samsonov, "High-Temperature Materials: Properties Index," Plenum Press, New York, 1964, pp. 96, 100-01.

(127) -128X


DAT
FILM